

Exploration of the new island of asymmetric fission

I. Tsekhanovich¹, A.N. Andreyev^{2,3}, K. Nishio³, D. Denis-Petit⁴, K. Hirose³, H. Makii³,
Z. Matheson⁵, K. Morimoto⁶, K. Morita^{6,7}, W. Nazarewicz⁵, R. Orlandi³, J. Sadhukhan^{8,9},
T. Tanaka^{6,7}, M. Vermeulen³ and M. Warda¹⁰

¹CENBG, CNRS/IN2P3-Université de Bordeaux, 33170 Gradignan, France

²Department of Physics, University of York, York YO10 5DD, United Kingdom

³Advanced Science Research Center, Japan Atomic Energy Agency, Tokai, Ibaraki 319-1195
Japan

⁴CENBG, CNRS/IN2P3, 33170 Gradignan, France

⁵Department of Physics and Astronomy and FRIB Laboratory, Michigan State University, East
Lansing, Michigan 48824, USA

⁶RIKEN Nishina Center for Accelerator-Based Science, Saitama 351-0198, Japan

⁷Department of Physics, Kyushu University, Fukuoka 819-0395, Japan

⁸Variable Energy Cyclotron Centre, Kolkata 700064, India

⁹Homi Bhabha National Institute, Mumbai 400094, India

¹⁰Institute of Physics, Maria Curie-Skłodowska University, 20-031 Lublin, Poland

Abstract

Fission properties of ^{178}Pt have been studied at the JAEA tandem accelerator in a complete fusion-fission reaction $^{36}\text{Ar} + ^{142}\text{Nd}$. The obtained fission-fragment mass – kinetic energy data are indicative of a mixture of the mass-asymmetric and mass-symmetric fission modes associated with different kinetic energies of the fragments. This constitutes the first observation of a multi-modal fission in the sub-Pb region. The measured fragment yields are dominated by asymmetric mass splits, with the symmetric mode contributing at the level of $\sim 1/3$. The experimental findings are well reproduced by the advanced density functional theory calculations.

1. Research Objectives

An experimental program aimed at studies of fission properties of nuclei in the region of extremely proton-rich nuclei below lead was initiated at the JAEA tandem facility. The interest to this region has raised after the unexpected observation of an asymmetric fragment-mass distribution (FFMD) in the β -delayed fission of ^{180}Tl , in which the daughter nucleus ^{180}Hg fissions in fragments with masses $A_1 \approx 100$ and $A_2 \approx 80$ [1], instead of the expected energetically preferred split into two semi-magic ^{90}Zr nuclei. Followed up experimental (cf. Ref. 2) and theory [3] efforts have shown a presence of an extended island of nuclei fissioning asymmetrically (see

Fig.1). The main objective of the present Reimei project was to probe the extents of the asymmetric fission region, by measuring FFMD for a series of $N=100$ isotones (^{180}Hg , ^{179}Au , ^{178}Pt and ^{177}Ir) created at low (below 20 MeV) excitation energies. The shape of the experimental FFMDs is of special interest for theory: it carries information about the interplay between symmetric and asymmetric mass splits and thus reflects importance of shell effects acting at large nuclear deformations. The symmetric and asymmetric fission modes are well known to co-exist and to compete in the region of actinides but so far they have never been observed

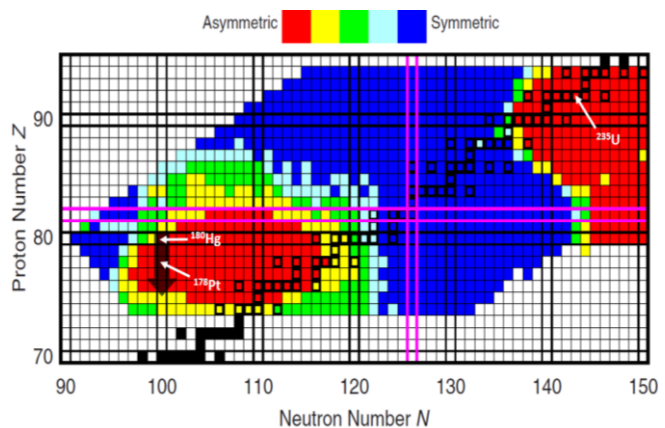


Fig 1 : Fragment-yield systematics for nuclei with $73 < Z < 95$ and $89 < N < 151$ adopted from [3]. The color code indicates different ratios (top of the figure) of the symmetric-to-asymmetric components in the expected MDs. The pointing down arrow goes through the nuclei to study.

experimentally in fission of nuclei below lead. In addition to that, fission of very exotic proton-rich matter provides an excellent tool to study the isospin dependence of the fission mechanism, which is of importance for testing models relevant to astrophysical scenarios (creation of elements in Supernova and neutron star merger events).

2. Research Contents

To explore the fission properties of nuclei in the new island of asymmetric fission, it is essential to create those nuclei at lowest possible excitation energies, which can be attained in fusion reactions with semi-magic $N=50$ beam bombarding nearly equal-mass targets (^{90}Zr , ^{89}Y , ^{88}Sr , ^{87}Rb). The availability of the ^{90}Zr beam and of the comprehensive fission setup makes of the JAEA the most suitable (unique) facility for the outlined research program. The initial Reimei proposal thus suggested to produce the nuclei of interest (^{180}Hg , ^{179}Au , ^{178}Pt and ^{177}Ir , cf. Fig.1) in complete fusion reactions of ^{90}Zr with $N=50$ targets, and the corresponding beam-time request received a full support from the JAEA tandem PAC. Nevertheless, the outlined measurements could not be conducted during the year 2017, due to some technical problems related to the tandem HV system. We have therefore made use of the asymmetric fusion reaction $^{36}\text{Ar} + ^{142}\text{Nd}$ having lower Coulomb barrier and thus requesting lower terminal voltage, to create ^{178}Pt (tough at higher excitation energies: $39 \text{ MeV} < E_{\text{CN}} < 59 \text{ MeV}$) and to study its fission properties.

Fission fragments of ^{178}Pt were detected with a two-arm time-of-flight (TOF) setup, with TOF arms positioned at $\pm 60^\circ$ relative to the beam axis. Each TOF arm was comprised of a micro-channel plate (MCP) based detector and a position-sensitive multi-wire proportional counter (MWPC), providing timing START and STOP signals, respectively. In order to cleanly distinguish between fission and scattered events, in addition to the TOF data, we made use of the energy deposited by charged particles in the MWPC detectors, as described in Ref. 4. For

every identified fission event, FF velocities in the laboratory (LAB) frame were derived from the measured TOF values and the FF positions in the MWPC and then converted to the center-of-mass (CM) frame. The resulting FF CM velocities were calibrated with the scattered beam, as well as corrected for attenuation in the target and TOF detectors.

The mass numbers A_1 and A_2 of complementary FFs, and their total kinetic energy (TKE), can be derived from the fragments' CM velocities v_1 and v_2 , under assumption of no particle emission (i.e., $A_1 + A_2 = A_{CN}$) from the compound nucleus A_{CN} during the pre-fission stage: $A_1 \cdot v_1 = A_2 \cdot v_2$ and $TKE = 0.5 A_{CN} \cdot v_1 \cdot v_2$. Figure 2b displays the correlation between TKE and fragment-mass data. Projection of Fig. 2b on the Y-axis gives the TKE distribution (Fig. 2a), whereas the projection on the X-axis delivers the FFMD (see Figs. 2e-g).

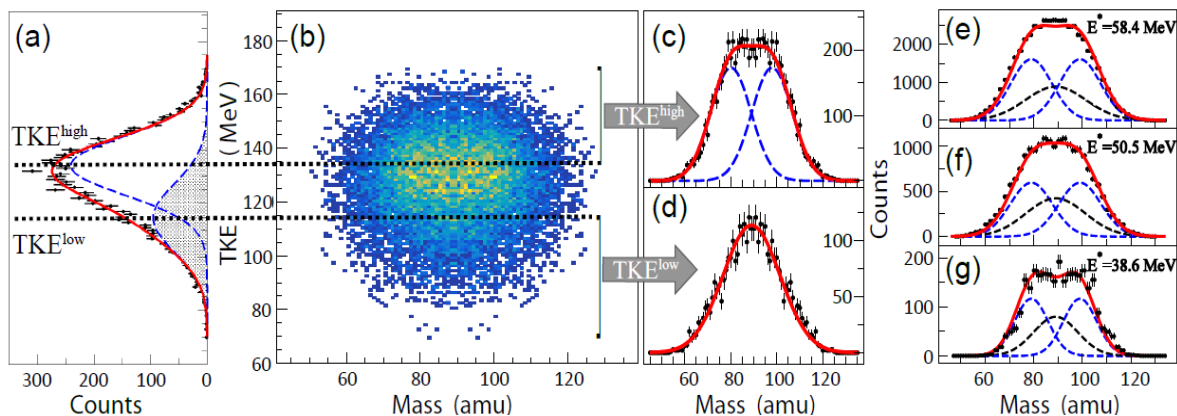


Fig 2 : (a) TKE distribution for $E_{beam} = 170$ MeV (projection of (b) onto the TKE-axis) de-convoluted into two components with derived positions of TKE^{high} and TKE^{low} , shown by dotted horizontal lines, see text for details. (b) TKE - FF mass correlation. TKE scale is identical for both (a) and (b). Mass spectra gated on events above TKE^{high} (c) and below TKE^{low} (d) fitted with a double- and single-Gaussian unconstrained function; fit results given by red lines. (e-g) Total FFMDs at different CN excitation energies. Solid red lines result from a fit with fixed symmetric and asymmetric mode positions as determined in (c) and (d). Blue and black dashed lines show the asymmetric and symmetric fit components, respectively. Experimental mass resolution is $\sigma_{exp} = 2.9$ amu.

3. Research results

It follows from Fig. 2a that the TKE distribution obtained for $E_{beam} = 170$ MeV is clearly skewed; similarly-skewed TKE distributions were obtained also at $E_{beam} = 155$ and 180 MeV. Therefore, a two-Gaussian fit was carried out to describe the TKE data. This fit, statistically reliable only at the two higher energies, yields two TKE components placed at TKE^{low} (maximum of the shadowed-area curve in Fig. 2a) and TKE^{high} (maximum of the other dashed curve), which are linked to the symmetric and asymmetric fission modes. This is demonstrated by the shape of the partial MDs constructed with events in Fig. 2b in the regions below TKE^{low} and above TKE^{high} and projected on the mass axis: narrow and clearly symmetric in Fig. 2d and wide and flat-top in Fig. 2c. The best-fit description of the partial MDs is correspondingly achieved with

one- and two Gaussians; they determine the light ($A_1 = 79(1)$ amu) and heavy ($A_2 = 99(1)$ amu) FF peak positions in the experimental total FFMDs (black circles in Figs. 2e-g).

Consequently, the FFMDs in Figs. 2e-g were fitted with a function composed of three Gaussians with fixed positions as obtained in Figs. 2c-d; the fit results shown with solid red and dashed lines. Overall, a good description of the experimental data is achieved. The asymmetric mode is found to be dominant, in accordance with theory. The weight of the symmetric mode amounts to $\sim 31\%$ at the three measured energies, as can be deduced directly from Figs. 2e-g. Thus, in contrast to actinides [5], the symmetric-mode contribution to the FFMDs does not significantly change with excitation energy. This can be explained in terms of the energy considerations: corrections to the excitation energy E_{CM} due to possible pre-fission neutron emission, rotational energy of the CN and the rotation-dependent fission-barrier height reduce the initial spread of 20 MeV in E_{CN} , resulting in practically identical (~ 25 MeV) effective excitation energy.

To interpret experimental results, nuclear density functional theory (DFT) calculations have been performed within two Hartree-Fock-Bogolyubov frameworks employing the Skyrme UNEDF1-HFB [6] and Gogny D1S [7] energy density functionals (cf. Fig. 3 for UNEDF1-HFB). Both approaches yield very similar picture of potential-energy surfaces (PES) and deliver the static fission path (solid red line in Fig.3) leading to the mass-asymmetric $A_1/A_2 \approx 80/98$ split, thus reproducing the experimental result. This path evolves on a fairly flat landscape, in contrast to a typical situation in heavy actinides (see e.g. [8, 9]). Absence of any ridge in the area of low octupole moments, along with a small

energy difference between the asymmetric and symmetric paths, suggests a possibility for a competition between different fission modes. At present, a detailed description of this competition is difficult to assess theoretically, as the post-scission configurations associated with fission valleys enter the picture and produce a sudden drop in PES at very large elongations (cf. Fig. 3), which makes it practically impossible to follow adiabatically the original fission trajectory. Interesting that competing fission pathways involving similarly asymmetric, compact, or elongated

shapes have also been predicted for multimodally fissioning nuclei in the fermium region [10, 11], i.e., for nuclei with much larger values of A_{CN} and much higher isospin.

Figure 3 also displays the nucleon localization functions (NLFs) [12] in pre-fragments (clusters connected with a neck) along the two fission pathways: asymmetric (ABCD) and symmetric (ABcd). Based on the analysis of NLFs, the asymmetric pre-scission configurations marked ‘‘C’’

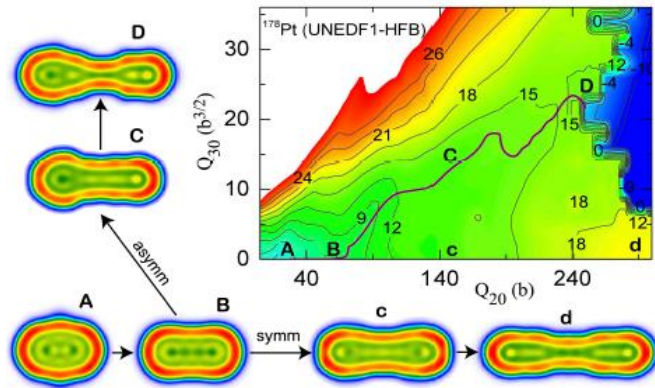


Fig 3 : PES of ^{178}Pt in the (Q_{20}, Q_{30}) plane calculated in UNEDF-HFB. The thick line indicates the static fission path obtained by the local PES minimization. Neutron localization functions illustrate various intrinsic configurations along the asymmetric (ABCD) and symmetric (ABcd) paths.

and “D” in Fig. 3 are composed of a nearly-spherical cluster around ^{86}Sr and a lighter deformed pre-fragment, resulting in FFs around ^{98}Mo and ^{80}Kr . In the symmetric configuration “c”, the pre-fragments can be associated with spherical ^{64}Ni nuclei.

Experimentally, we find that both symmetric and asymmetric fission modes follow the trend previously observed in heavier, trans-lead nuclei [13]. In particular, higher values of TKE in the asymmetric mode -- which also match well the $\text{TKE}=135.9\text{MeV}$ value expected from the Viola systematics [14] -- are indicative of less deformed scission configurations, whereas for the symmetric mode, highly elongated FF shapes are expected from its lower TKE values. This finding is consistent with the shapes of nucleon localizations shown in Fig. 3: symmetric configuration “d” corresponds to highly deformed fragments without a well-defined neck.

4. Conclusion

The FFMDs of ^{178}Pt produced in a complete fusion reaction $^{36}\text{Ar} + ^{142}\text{Nd}$ are found to be predominantly asymmetric, with the most probable mass division $A_1\approx 79$ and $A_2\approx 99$, which is also reproduced by the DFT calculations. The combined analysis of the FFMDs and TKE distributions made it possible to separate asymmetric and symmetric fission modes. It is found that the asymmetric mode is associated with larger TKE values than the symmetric mode. Moreover, its average TKE follows the systematics [14] established for actinides, which suggests the asymmetric mode's insensitivity to the isospin of the CN, at least for $A_{\text{CN}} > 177$.

The present work provides new experimental information on the extension of the recently-discovered island of asymmetric fission towards lower atomic numbers. For the first time, the interplay between different fission modes has been found in a nucleus from the sub-lead region. This provides strong motivation for extending microscopic models of fission to FFMDs and TKE distributions at nonzero excitation energies, as well as for addressing the question of possible interferences between asymmetric and symmetric fission modes.

5. References

- [1] A. N. Andreyev *et al.*, **Phys. Rev. Lett.**, 105, 252502, (2010).
- [2] A. N. Andreyev, K. Nishio, and K.-H. Schmidt, **Rep. Prog. Phys.** 81, 016301 (2018).
- [3] P. Moller and J. Randrup, **Phys. Rev. C** 91, 044316 (2015).
- [4] K. Nishio *et al.*, **Phys. Lett. B** 748, 89 (2015).
- [5] C. Straede, C. Budtz-Jorgensen, and H.-H. Knitter, **Nucl. Phys. A** 462, 85 (1987).
- [6] N. Schunck *et al.*, **J. Phys. G** 42, 034024 (2015).
- [7] J. Berger, M. Girod, and D. Gogny, **Comput. Phys. Commun.** 63, 365 (1991).
- [8] J. D. McDonnell *et al.*, **Phys. Rev. C** 90, 021302 (2014).
- [9] T. Ichikawa *et al.*, **Phys. Rev. C** 86, 024610 (2012).
- [10] M. Warda *et al.*, **Phys. Rev. C** 66, 014310 (2002).
- [11] A. Staszczak *et al.*, **Phys. Rev. C** 80, 014309 (2009).
- [12] C. L. Zhang, B. Schuetrumpf, and W. Nazarewicz, **Phys. Rev. C** 94, 064323 (2016).
- [13] Y. L. Zhao *et al.*, **Phys. Rev. Lett.** 82, 3408 (1999).
- [14] V. E. Viola, K. Kwiatkowski, and M. Walker, **Phys. Rev. C** 31, 1550 (1985).